



Geochemistry and petrogenesis of basic Paleogene volcanic rocks in Alamut region, Alborz mountain, north of Iran

Mehdi Nazari Sarem¹, Mansour Vosoghi Abedini¹, Rahim Dabiri^{2*}, Mohammad Reza Ansari³

1. Department of Geology, Tehran Science and Research Branch, Islamic Azad University, Tehran, Iran.

2. Department of Geology, Mashhad Branch, Islamic Azad University, Mashhad, Iran.

3. Associate Professor, Department of Geology, Chalous Branch, Islamic Azad University, Chalous, Iran.

*Corresponding author: Rahimdabiri@yahoo.com

ABSTRACT

The activities of Alborz Tertiary magmatism are mainly attributed to the subduction and closure of Neo-Tethys. These phenomena, including the magma origin of this lesser area, are investigated in this study. In addition, the origin of the magma characteristics based on the geochemistry of main and rare elements is also studied, and a model is presented for their tectonomagmatic status. Volcanic Tertiary Alamut is part of magmatism in the central Alborz-west sequence of volcanic rocks (including basalt, trachyandesite, and basaltic andesite with alkaline geochemical properties, with porphyritic texture, pyroclastic rocks, and volcanic breccia) directly above the units belongs to the Karaj Formation (Middle Eocene age). Geochemical properties indicate that the parent magma is characterized by high ratios of LREE/HREE as well as Th/Nb, La/Nb, Ba/Nb, Zr/Nb, and low K/Nb ratios. The early basaltic magma is formed from a garnet lherzolite mantle by phlogopite/pargasite metasomatism at 2.5-5.3 GPa and depths of more than 80-150 km. Structural evidence suggests the formation of these volcanic rocks in a continental rift zone setting. The appearance of these rocks can be attributed to the effects of intercontinental extensional phases in deep faults during Eocene Alpine orogeny phases. The primary focus of this study is to provide the geological, petrographical, and geochemical data findings of the volcanic basaltic rocks along with the results of studying other rocks in this region. Aside from the mode and their formation, magma forming is also investigated. Moreover, for the rocks investigated in this study, the environment and the site of the tectonic-magmatic region are also clarified in detail.

Keywords: Geochemical modeling; Central Alborz; Petrology; Paleocene;

Geoquímica y petrogénesis de las rocas volcánicas básicas del Paleógeno en la región de Alamut, montaña de Alborz, norte de Irán

RESUMEN

Las actividades del magmatismo terciario en Alborz (Irán) se atribuyen principalmente a la subducción y final del neotetis. Este fenómeno es el objeto de este estudio, además de un acercamiento al origen del magma de esta área inferior. Adicionalmente, los autores estudiaron las características y origen del magma con base en la geoquímica de los elementos principales y de las tierras raras, y presentaron un modelo de su estado tectonomagmático. El terciario volcánico de Alamut es parte del magmatismo en la secuencia central de rocas volcánicas en Alborz occidental (incluye basalto, traquiandesita, y andesita basáltica con propiedades geoquímicas alcalinas, con textura porfirítica, rocas piroclásticas y brecha volcánica), directamente sobre las unidades pertenecientes a la Formación Karaj (del Eoceno medio). Las propiedades geoquímicas indican que el magma madre se caracteriza por altos índices de elementos tierras raras ligeros y elementos tierras raras pesados, al igual que proporciones torio/niobio, lantano/niobio, bario/niobio, circonio/niobio y menormente potasio/niobio. El magma basáltico temprano está formado por un manto de lherzolitas de granate con metasomatismo flogopita/pargasita a 2.5-5.3 Gpa y profundidad entre 80 y 150 kilómetros. La evidencia estructural sugiere la formación de estas rocas volcánicas en un ambiente de grieta continental. La aparición de estas rocas puede atribuirse a los efectos de las fases extensionales intercontinentales en fracturas profundas durante las fases orogénicas del Eoceno alpino. El enfoque principal de este estudio es proporcionar la información hallada en términos geológicos, petrográficos y geoquímicos de las rocas volcánicas basálticas al igual que los resultados del análisis de otras rocas en el área. Más allá de su modo y formación, los componentes del magma también se analizaron. Además, para las rocas investigadas en este estudio, el ambiente y el sitio de la región tectonomagmática se aclararon detalladamente.

Palabras clave: modelo geoquímico; Alborz central; petrología; Paleoceno;

Record

Manuscript received: 04/08/2019

Accepted for publication: 12/11/2019

How to cite item

Nazari Sarem, M., Vosoghi Abedini, M., Dabiri, R., & Ansari, R. A. (2021). Geochemistry and petrogenesis of basic Paleogene volcanic rocks in Alamut region, Alborz mountain, north of Iran. *Earth Sciences Research Journal*, 25(2), 237-245. DOI: <https://doi.org/10.15446/esrj.v25n2.74025>

Introduction

A key feature of alkaline volcanic rock compounds in the continental regions is their incompatible enrichment of elements, mainly volcanic, depending on the final stages of the active subduction zones of continental margins. These properties are transmitted to magmas that have passed through an enrichment continental crust of incompatible elements and can later be observed with contaminated crust (Wilson, 1989). Concerning the mantle origin, volcanic regions of the post-orogenic areas have been proposed in previous studies, including the continental lithosphere enriched by materials released from the oceanic plate (Lima and Nardi, 1998), asthenosphere plumes from deep areas, the mantle (Lei and Zhao, 2007) or the participation of both of them (Pearce et al. 1990; Turner et al., 1992). Tertiary mafic volcanic rocks in northern Alborz Iran are believed to be the result of subduction of Neo-Tethys (Stalder, 1971; Alavi 1996; Hasanzadeh 2004). In Eocene, due to the subduction of Neo-Tethys, a back-arc basin is formed. The crust tensional stress results in the subsidence generating the current southern Alborz (Burberry and King, 1981). The region's tensile behavior in Eocene causes the flow of high thermal magmatism influencing all Neo-Tethys subduction zones, such as East Iran and southern Alborz (other than northern Alborz and Kopet Dagh) (Vincent et al., 2005). Due to the rollback of the intrusive oceanic plate in Eocene and the removal of pressure, the melting liquid lithosphere mantle and the asthenosphere rise. This asthenosphere uplift and the thinness of the crust produce large amounts of volcanic rocks in the Eocene of Alborz. The combination of these rocks often shows rare mantle elements (Verdel, 2009). However, studies and information on the origin of these volcanic activities are pretty limited. By considering the characteristics of the origin of these magmas, the current study presents a tectonomagmatic model for these magmatic activities.

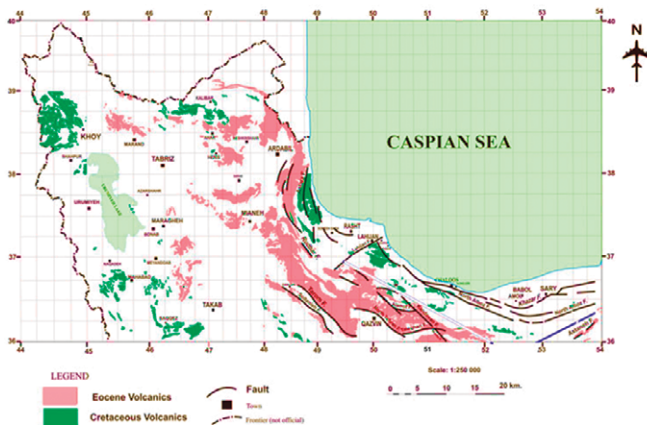


Figure 1. Map of Cretaceous and Eocene volcanic outcrops in Alborz, based on Qazvin's quadrilateral maps of Rasht.

Geological setting

The study area is located in the central parts of the Alborz Mountains structural zone in Qazvin Province in Iran (Fig. 1). Alamut region is situated between $50^{\circ} 02' 54''$ and $50^{\circ} 52' 55''$ as well as from $36^{\circ} 17' 11''$ to $36^{\circ} 41' 01''$ northern latitudes. The area is divided into two parts of Western Rudbar Alamut and Eastern Rudbar Alamut. There exist the oldest outcrops of Paleozoic rocks in the region, including chert dolomitic rocks with Zagon mica shale, sandstone, and limestone. The Mesozoic rock units include a series of dark gray shale with sandstone layers. The rock units' outcrops in the Eocene period include a series of dark volcanic rocks with basaltic to andesitic composition along with faultly fractured altered andesitic tuff and hyaloclastite breccia. An alternative collection of green tuff, tuffite, crystalline tuff, sandstone tuff, calcareous tuff, marl, shale, and lava parts with andesitic dacite to rhyodacite composition appears in the north of the Anke-Barajin trust fault (North Qazvin fault). Essential outcrops of rock units have been formed during the Neogene, from dark to brown volcanic rocks with trachyte, andesitic dacite composition, and local feldspathoid volcanic lava.

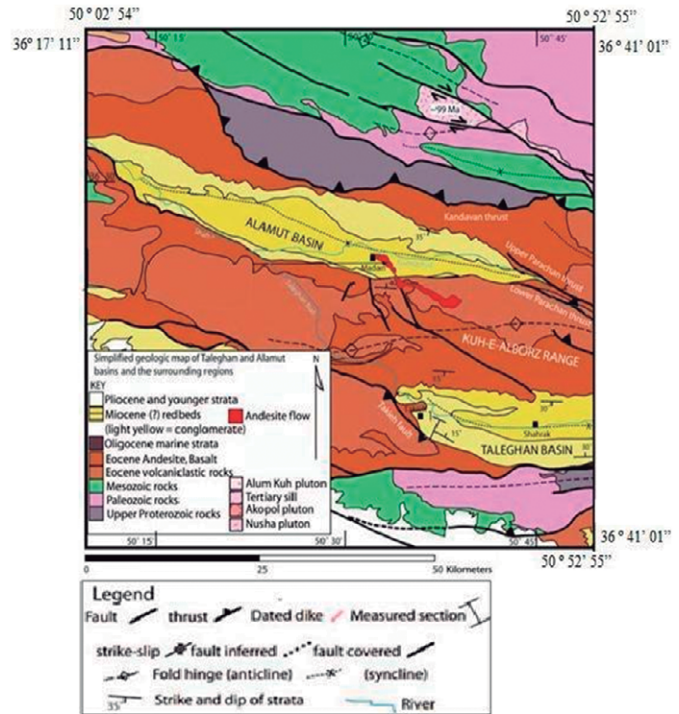


Figure 2. Simplified geologic map showing regional geology of the central Alborz (Alamut basins) (after Guest et al., 2007).

Samples and Methods

The present study was based on field studies, petrography, and chemical analysis of main and rare elements. Field studies investigated the area of study in terms of lithology and sampling. In this regard, for the litho-geochemical studies, the macroscopic samples of volcanic rocks were selected and sent to Mashhad laboratory to produce thin sections. Ten suitable samples were sent to the ACME Laboratory in Canada to analyze the whole rock by the ICP method. Minpet, Excel, Petrography, GCDkit, and other specialized software were implemented to scrutinize the research findings. In the last stage of the research, field study, petrography, and geochemistry data were analyzed, and a comprehensive view was made on petrology, tectonics, and geochemistry status of the region.

Lithological study

According to the field and petrography studies, volcanic rocks of the region are constituted from intermediate to basic lava plus pyroclastic rocks of Eocene in a shallow marine environment with basaltic andesite, andesitic basalt, olivine basalt, and basalt composition. The dominant textures include porphyritic with microlithic matrix, porphyritic with medium grain matrix, and doleritic texture. According to mineralogy, the rocks are predominantly composed of plagioclase, clinopyroxene, and olivine. The textures in plagioclase in basaltic rocks include mainly sieve and glomerophytic textures. Plagioclase crystals contain polysynthetic, carlsbad, albite-pericline with defected and albitized margin. Fine olivine crystals are often subautomorph and altered into biotite, serpentine, chlorite, iron oxide, and iddingsite. The matrix comprises glass, plagioclase microliths, opaque minerals, and secondary minerals (Fig. 3).

Geochemical analysis of volcanic rocks

The results on the major elements of volcanic rocks in the Alamut region show that these rocks include a series of basic volcanic rocks. SiO_2 content in these rocks varies from 48.21 to 48.28 wt%. The rocks can be categorized into basaltic, trachybasaltic, and andesitic basaltic rocks based on

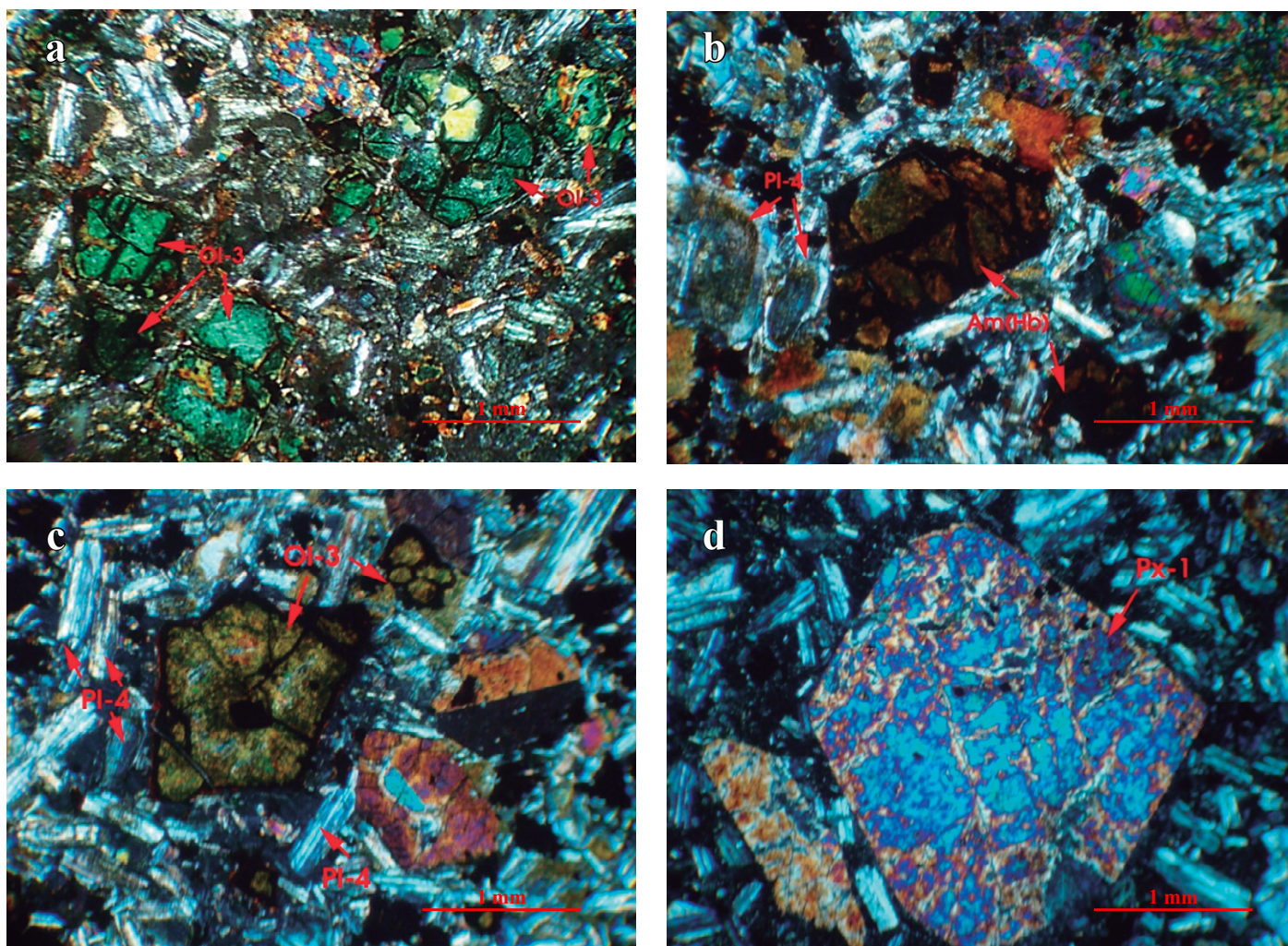


Figure 3. (a) A matrix enriched with sodic plagioclase in basalt, (b) porphyritic texture with microlithic glass matrix, chlorination of olivine in a matrix rich of sodic plagioclase in basalt, (c) porphyritic texture with microlithic glass matrix and the presence of clinopyroxene phenocrysts, (d) porphyritic texture with microlithic glass matrix, chlorinated olivine with clinopyroxene and plagioclase phenocrysts.

the TAS diagram (Figs. 4a and b). According to the sub-alkaline and alkaline series (Irvine & Baragar, 1971), the rocks fall in the alkaline range (Figs. 4c and d). The variations in the major elements are plotted versus MgO in Figure 5. The level of major oxides such as Al_2O_3 and SiO_2 increases with the reduction of MgO during magmatic differentiation. At the same time, the level of major oxides such as CaO and Fe_2O_3 drops with the reduction of MgO. The magnesium number (Mg#) of samples varies from 30 to 45. Most samples have a high Mg# in the range of the parent magma. Two samples with an Mg# of less than 40 and a far lower level of mid-plate basalts (as those found in Hawaii) are comparable with continental flood basalts (CFB) and rift basalts (similar to those found in the Rio Grande) with low to moderate magnesium numbers lacking characteristics of primitive mantle lava (Raymond, 2002). Variation of minor elements versus Zr and Th is one of the proper approaches to characterize magmatic transformations. Zr is used in these diagrams mainly due to the very low mobility of this element during alteration (Le Roex et al., 1983; Meng et al., 2012; Talusani, 2010; Widdowson et al., 2000; Widdowson, 1991) and a wide range of variations of this element in basaltic rocks. In addition, Zr shows a completely incompatible geochemical behavior during partial melting and differential crystallization of basaltic lavas (Talusani, 2010) and tends to enter and remain in the melt phase. As seen in Figure 6, Ni is slightly scattered positive versus Zr, and Th is somewhat scattered positive versus Hf. The trends observed in these diagrams represent that the rocks in this region have nearly similar geochemical characteristics with their source magma. In

addition, the crystallization process plays the main petrological role in the basaltic magma evolution in the region. However, scattering can be attributed to the frequency of mafic and plagioclase phenocrysts. For further analysis of geological processes and the original characteristics of the basaltic rocks, the normalized pattern of the average values of rare and rare earth elements in basalts was plotted versus chondrites, the primitive mantle, and depleted mid-oceanic ridge basalts and was then compared with OIB, EMORB, and NMORB patterns (Fig. 7). No particular Eu anomaly is observed in a diagram normalized relative to the chondrite values. This can be attributed to the lack of plagioclase and clinopyroxene differentiation (Zeng et al., 2010) during the magma evolution of forming the rocks in the region. A negative anomaly in Nb indicates the role of magmatic contamination with continental crust in the evolution of rocks. Severe positive Pb and Ba anomaly has been reported for continental crust contamination, with the positive Sr anomaly indicating the presence of plagioclase phenocrysts in the rock. More than 10 times enrichment of light rare earth elements (LREE) in comparison with heavy rare earth elements (HREE) in most samples suggests that garnet does not enter the melt but remains in the mantle origin. As can be seen, the average value of minor elements and the rare earth elements in basalts (AVS) show a pattern between EMORB and OIB with a similar general pattern. The normalized pattern of the samples is located between EMORB and OIB; hence the source of basalts in this region is confirmed by characteristics of these two origins. Although both of them have originated from the asthenosphere mantle, they may have also been affected by the lithospheric mantle to some extent.

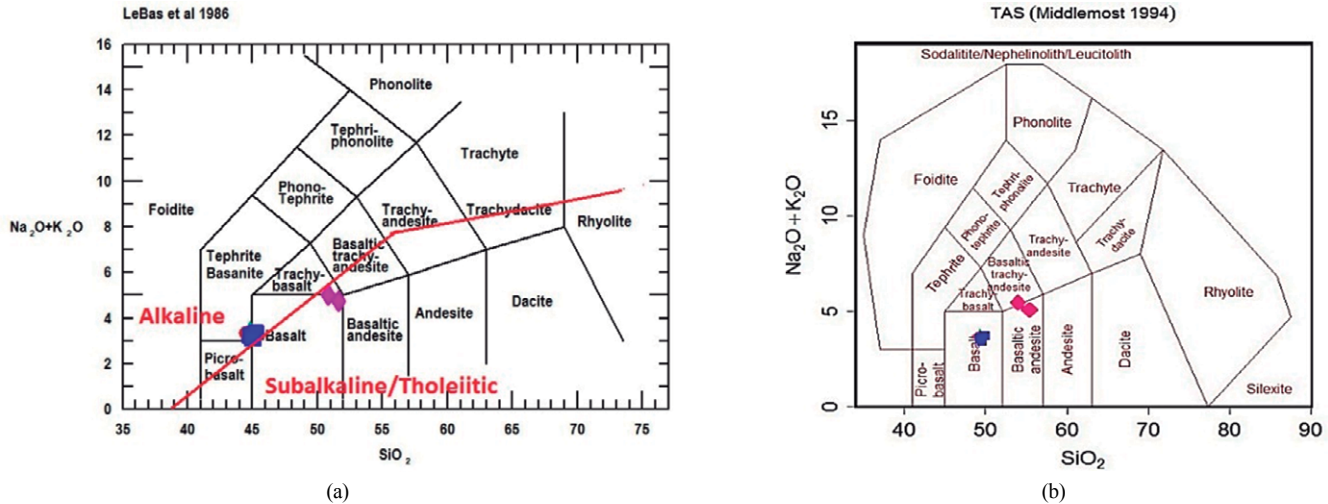


Figure 4. (a) $\text{Na}_2\text{O} + \text{K}_2\text{O}$ versus SiO_2 (Le Bas et al., 1986); and (b) $\text{Na}_2\text{O} + \text{K}_2\text{O}$ versus SiO_2 (Middlemost, 1994)

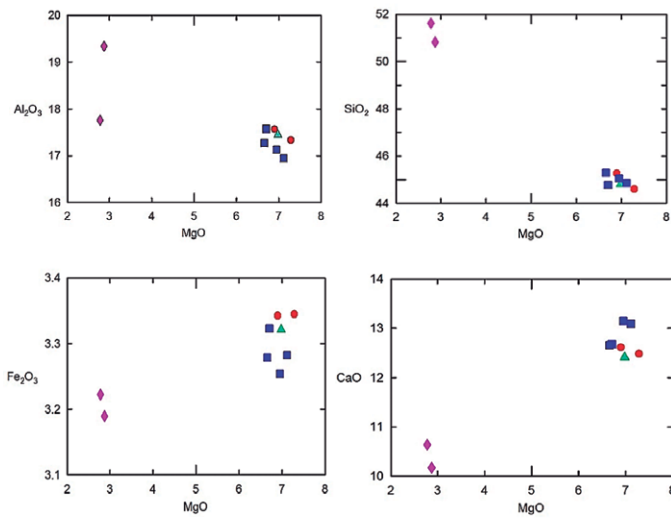


Figure 5. Variation diagrams of the major elements versus MgO

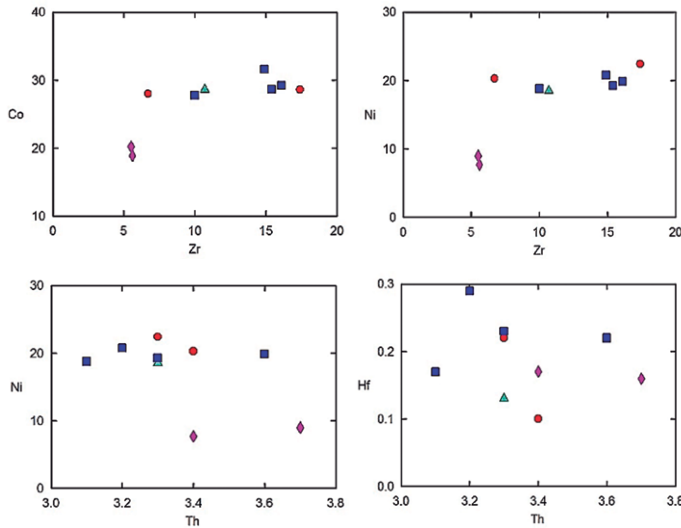


Figure 6. Variation diagrams of incompatible elements

The similarity of basalts pattern in the region to ocean island basalts (OIB) rather than enriched mid-ocean ridge basalts (EMORB) can be explained by the fact that the main origin of these basalts is partially enriched asthenosphere mantle similar to the OIB origin. Despite the similarity of pattern of both groups, varieties of Alamut basalts in the elements Sr, Nb, and Zr show less enrichment than varieties of OIB. This geochemical difference can be explained by degrees of partial melting. Sometimes, the enrichment of partial melting in the rocks of the region can lead to element depletion (such as light rare earth elements) causing a lower concentration of incompatible elements and providing a lower slope of distribution for these elements as compared to OIB. An important point that needs to be taken into consideration is the high value of the Zr/Hf ratio with an average of around 60.67. According to Wever et al. (2003) and Tappa (2004), high Zr/Hf ratios reflect a residual clinopyroxene phase and lack of clinopyroxene under melting conditions. Their findings suggest that Hf with a coefficient of 1.5-2 times is more compatible than Zr in clinopyroxene mineral in the melt/clinopyroxene system.

According to the results, the mantle source of the AVS parent magma is depleted in Hf as compared with Zr, hence the high ratio of Zr/Hf could be attributed to the low degree of partial melting (Daviid et al., 2000). Therefore, it appears that besides lower partial melting which reflects the great depths of the parent mantle, the metasomatism of the parent mantle and its heterogeneity in the production of such melt can be considered as the primary source. The steep slope of HREE/LREE in the diagrams is an indicator of the presence of the garnet phase in the mantle source. In such conditions, for alkaline basalts, a deep source of garnet lherzolite with phlogopite/pargasite (mantle hornblende) at 2-2.5 GPa pressure is recommended (Thirlwall et al., 1994; Tappa 2004; Stivenson 2003; Glasser et al., 1999). From the normalized graphs of Alamut volcanic rocks based on spider diagrams, it could be concluded that due to the low K / Nb ratio and the enrichment of regional rocks with light rare earth elements (LREE) relative to heavy rare earth elements (HREE), the alkaline magma of these rocks has originated from low grade melting from a rich mantle source.

Plots of Sm/Yb versus La/Yb and La/Yb versus Dy/Yb are usually employed to detect peridotite spinel from garnet peridotite melting. In general, Yb is compatible with garnet, while La and Sm are incompatible. Accordingly, Sm/Yb and La/Yb are significantly concentrated in garnet peridotite origin at low degrees of partial melting. In contrast, during partial melting in the stability range of spinel, the La/Yb ratio is only slightly altered, but the Sm/Yb ratio remains almost unchanged (Xu et al., 2005; Yaxley, 2000; White & Mckenzi, 1995). In the diagram designed by Lai et al., (2012) based on the Sm/Yb ratio versus La / Yb, the basaltic samples of the region are located within the range of 12 to 15% of the garnet peridotite range (see Fig. 8 a and b).

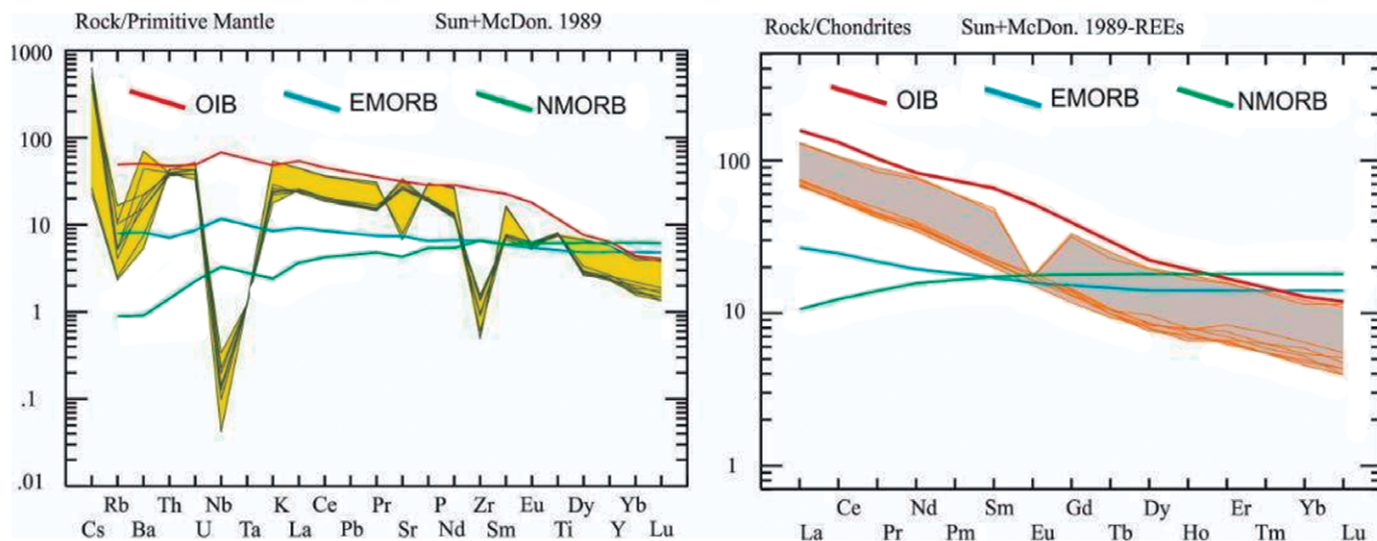


Figure 7. (a) spider diagram normalized to primitive mantle values (Sun and Mc Donough, 1989), (b) spider diagram normalized to primitive mantle values. (Wood et al., 1979), (c) spider diagram normalized to OIB (Sun and Mc Donough, 1989).

Table 1. Results of chemical analysis of the oxides of the main and secondary elements by the ICP of volcanic rocks in the Alamut area

Sample	6845 -a120	6846 -a110	6847 -a130	6848 -a140	6849 -a116	6850 -a150	6851 -a128	6852 -a151	6853 -a117B
SiO ₂	50.82	44.77	44.80	44.61	45.26	44.85	45.29	45.05	51.62
Al ₂ O ₃	19.35	17.58	3.34	17.34	17.56	16.95	17.28	17.12	17.77
Fe ₂ O ₃	3.19	3.33	3.33	3.34	3.34	3.28	3.28	3.26	3.22
Feo	6.16	9.31	9.20	9.07	8.54	9.12	9.13	9.03	6.82
MgO	2.88	6.71	6.98	7.29	6.90	7.12	6.66	6.95	2.77
CaO	10.17	12.67	12.43	12.49	12.62	13.08	12.65	13.15	10.64
Na ₂ O	3.42	2.56	2.89	2.67	2.62	2.44	2.65	2.21	3.12
K ₂ O	1.63	0.69	0.54	0.67	0.74	0.79	0.72	0.873	1.61
TiO ₂	1.61	1.75	1.75	1.77	1.77	1.70	1.70	1.69	1.617
P ₂ O ₅	0.66	0.45	0.44	0.41	0.45	0.42	0.41	0.41	0.65
MnO	0.14	0.22	0.26	0.28	0.22	0.21	0.19	0.21	0.14
Cr ₂ O ₃	0.009	0.009	0.009	0.11	0.009	0.01	0.022	0.03	0.024
sum	99.23	99.37	85.26	99.3	99.4	99.3	99.3	99.3	99.187
K	13500.75	5779.50	4449.60	5518.14	6127.06	6637.12	6000.18	7249.21	13331.13
P	2857.77	1933.72	1880.75	1749.98	1932.86	1836.64	1783.11	1769.59	2803.66
Tl	9623.3	10434.5	10459.2	10563.5	10556.3	10217.0	10236.3	10158.7	9691.61
Mo	1.02	0.95	0.85	0.74	0.55	1.01	0.85	1.02	1.23
Cu	112.2	90.74	158.44	71.86	198.36	133.59	89.67	103.34	172.03
Zn	101.8	69.7	71.5	73.3	70	62.8	63.8	70	82.4
Ag	34	30	54	21	75	41	39	39	59
Ni	7.7	19.9	18.5	7.7	19.9	18.5	7.7	19.9	18.5
Co	18.9	29.2	28.6	28.6	28	27.8	28.7	31.6	20.2
Mn	850	1028	1359	1486	953	971	951	1009	904
Fe	5.59	6.29	6.67	6.01	6.04	5.92	6	6.34	6.01
As	1.1	0.3	0.8	0.7	1.4	1.4	0.8	1.2	0.9
U	0.9	1.1	0.8	0.9	0.9	0.8	U	0.9	1.1
Au	3	1.4	0.6	0.8	0.9	Au	3	1.4	0.6
Th	3.4	3.6	3.3	3.3	3.4	3.1	3.3	3.2	3.7
Sr	168.1	559.5	533	536.6	537.7	588.3	714.8	655.9	142.6
Cd	0.01	0.03	0.03	0.03	0.02	0.02	0.01	0.01	0.03
Sb	0.37	0.11	0.1	0.13	0.08	0.12	0.05	0.08	0.19

(Continue)

Table 1. Results of chemical analysis of the oxides of the main and secondary elements by the ICP of volcanic rocks in the Alamut area

Sample	6845 -al20	6846 -al10	6847 -al30	6848 -al40	6849 -al16	6850 -al50	6851 -al28	6852 -al51	6853 -al17B
Bi	0.02	0.02	0.02	0.02	0.02	0.02	0.02	0.02	0.02
V	186	204	233	222	211	190	198	205	185
Ca	3.44	3.56	3.52	2.96	3.44	3.67	3.5	4.02	4.09
La	30.6	17.8	17.2	16.4	17.6	16.2	16.6	16	31
Cr	16.6	30.3	38.3	65.4	37.2	34.2	35.6	44.2	17.1
Mg	1.32	1.84	1.96	1.86	1.88	1.95	1.81	2.01	1.37
Ba	52.4	131.6	151	109.5	306.8	107.7	491.3	155	37.6
B	20	20	20	20	20	20	20	20	20
Al	3.07	6.73	6.8	6.34	6.58	6.31	6.85	6.63	2.59
Na	0.419	1.388	1.592	1.473	1.418	1.323	1.565	1.178	0.34
W	0.07	0.51	0.05	0.12	0.05	0.11	0.13	0.17	0.07
Sc	14.9	3.9	3.7	3.8	4	3.9	3.8	3.5	16.6
S	0.02	0.02	0.02	0.02	0.02	0.02	0.02	0.02	0.02
Tl	0.02	0.02	0.02	0.03	0.02	0.05	0.03	0.06	0.02
Hg	10	6	5	11	12	5	9	10	5
Se	0.2	0.1	0.1	0.2	0.1	0.1	0.2	0.2	0.1
Te	0.02	0.02	0.02	0.02	0.02	0.02	0.02	0.02	0.02
Ga	9.4	12.3	12.8	12.2	12.5	11.6	12	12.3	8.8
Cs	0.21	3.28	5.03	4.31	4.06	4.05	3.97	2.99	0.18
Ge	0.2	0.1	0.1	0.1	0.1	0.1	0.1	0.1	0.2
Hf	0.17	0.22	0.13	0.22	0.1	0.17	0.23	0.29	0.16
Nb	0.07	0.16	0.09	0.14	0.03	0.1	0.1	0.24	0.07
Rb	1.6	2.6	3.5	3.3	3.3	6.5	6.9	10.6	1.5
Sn	1.4	1	0.9	0.8	0.7	0.8	0.9	0.8	1.5
Ta	0.05	0.05	0.05	0.05	0.05	0.05	0.05	0.05	0.05
Zr	5.6	16.1	10.7	17.4	6.7	10	15.4	14.9	5.5
Y	24.66	11.67	10.42	10.56	12.11	11	11.16	11.05	26.25
Ce	64	36.6	35.2	33.1	36.3	33.9	33.3	33.6	64.9
In	0.07	0.02	0.02	0.02	0.02	0.02	0.02	0.02	0.04
Re	1	1	1	1	1	1	1	1	1
Be	1.4	1.4	1.5	1.2	0.8	0.9	1.1	1.4	1.1
Li	5.7	25.7	37.9	33.2	37.6	22.5	25.1	17	6
Pr	7.97	4.3	4.23	4.01	4.64	4.07	4.2	4.22	8.53
Nd	35.41	18.02	17.16	16.11	18.54	17.59	16.94	16.95	36.56
Sm	7.38	3.25	3.31	3.04	3.44	3.24	3.42	3.25	7.06
Eu	0.99	0.95	0.95	0.88	1.06	0.95	1.02	0.96	1.01
Gd	6.5	2.98	2.68	2.41	2.92	2.83	2.71	2.86	6.79
Yb	1.94	1.09	0.81	1	0.92	0.89	0.84	0.77	2.07
Er	2.59	1.38	1.08	1.1	1.25	1.16	1.03	1.06	2.63
Lu	0.29	0.14	0.11	0.12	0.13	0.1	0.11	0.1	0.28
Pd	10	10	10	10	10	10	10	10	10
Pt	2	2	2	2	2	2	2		
Pb ₂ O ₇	1.32	0.97	0.77	0.78	0.9	0.9	0.86	0.78	1.41
Pb ₂ O ₈	3.3	2.42	1.88	1.93	2.28	2.24	2.14	1.94	3.47
Pb ₂ O ₄	0.08	0.06	0.05	0.05	0.06	0.06	0.05	0.05	0.09
ZR/HF	32.94	73.18	82.30	79.09	67	58.82	66.95	51.37	34.37

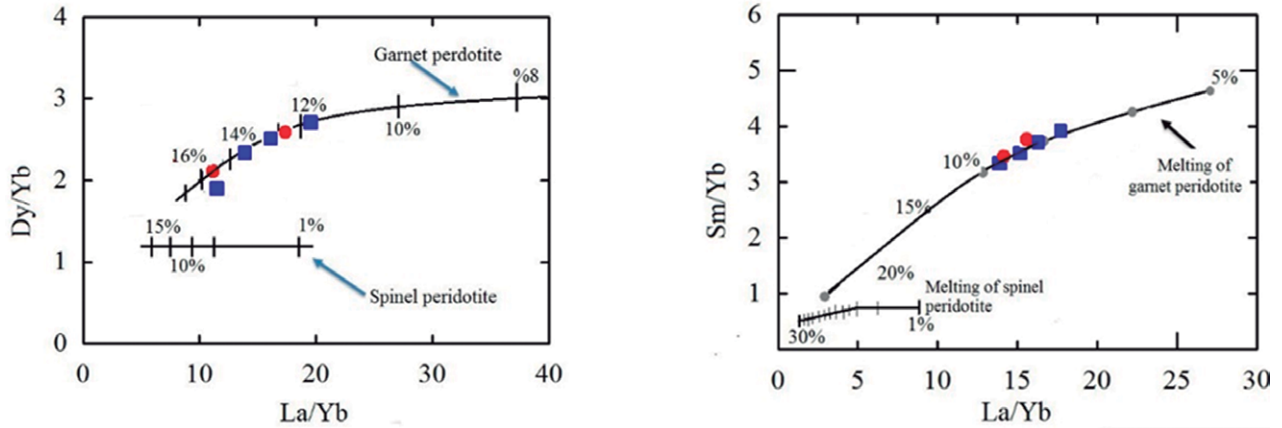


Figure 8. (a) Dy/Yb versus La/Yb from Thirlwall et al. (1994) and Bogaard et al. (2003), and (b) The logarithmic diagram of Sm/Yb versus La/Yb from Lai et al. (2012) for determining the degree of partial melting.

A variety of graphs have been implemented to determine the tectonic setting of the magma-forming rocks in the region. In the Ta/Hf versus Th/Hf diagram (Wang et al., 2001), the basalts in the study area fall within the range of extensional or primary rift environments. The alkaline properties of these rocks confirm their formation environment (Fig. 9-a). In the Ti/Y versus Zr/Y diagram (Pearce and Gale, 1977), the samples have been situated within the continental and continental margin ranges (Fig. 9-b). Finally, in the V versus Ti/1000 (Schervais, 1982) and Nb/Yb versus TiO₂/Yb diagrams, the samples are located in the OIB and alkali basalt ranges (Fig. 9).

Stratigraphic and structural studies by Allen et al. (2003) indicate that AMA volcanoclastic deposits have been formed during an extensional phase in the early Eocene. Asiabanha and Foden (2012) suggested that this extension occurred in a back-arc environment. Due to the basin uplift during the stress

regime in the late Eocene, the next volcanic phase has occurred in the sub-aerial phase form. According to the results, the following model can be used for the Eocene-Oligocene magmatic activity in the study area. This model is similar to the one proposed by Humphreys et al. (2003) for West America, which consists of four steps:

In the first stage, the steep oceanic crust subduction led to the formation of a volcanic arc in the north of the Arabian-Eurasia structural zone (Fig. 10-a). In the second stage, after the Aptian-Albian orogeny phase, the subduction continued with a lower slope causing magmatic activity in the north of Central Iran and Alborz. At the end of the Cretaceous period, some tectonic contractions occurred from Iran to the north of this structural zone. At this stage, upper mantle uplift occurred in Alborz and northern Iran mountains (Zaeimnin et al., 2011; Haghazari, 2012; Haghazari et al., 2015).

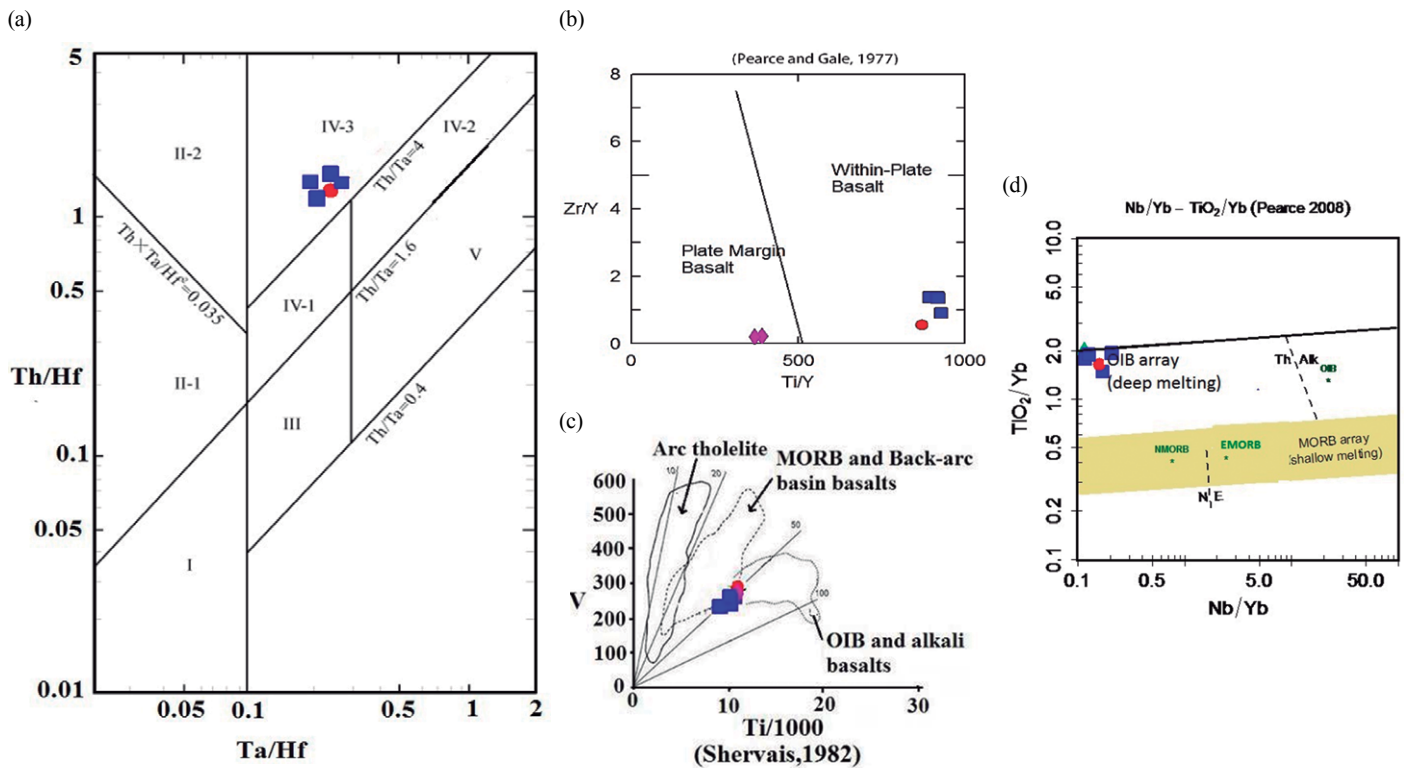


Figure 9. (a) Ta/Hf versus Th/Hf (Wang et al., 2001), (b) Ti/Y versus Zr/Y (Pearce and Gale, 1977), (c) V versus Ti/1000 (Schervais, 1982) and (d) Nb/Yb versus TiO₂/Yb (Pearce, 2008)

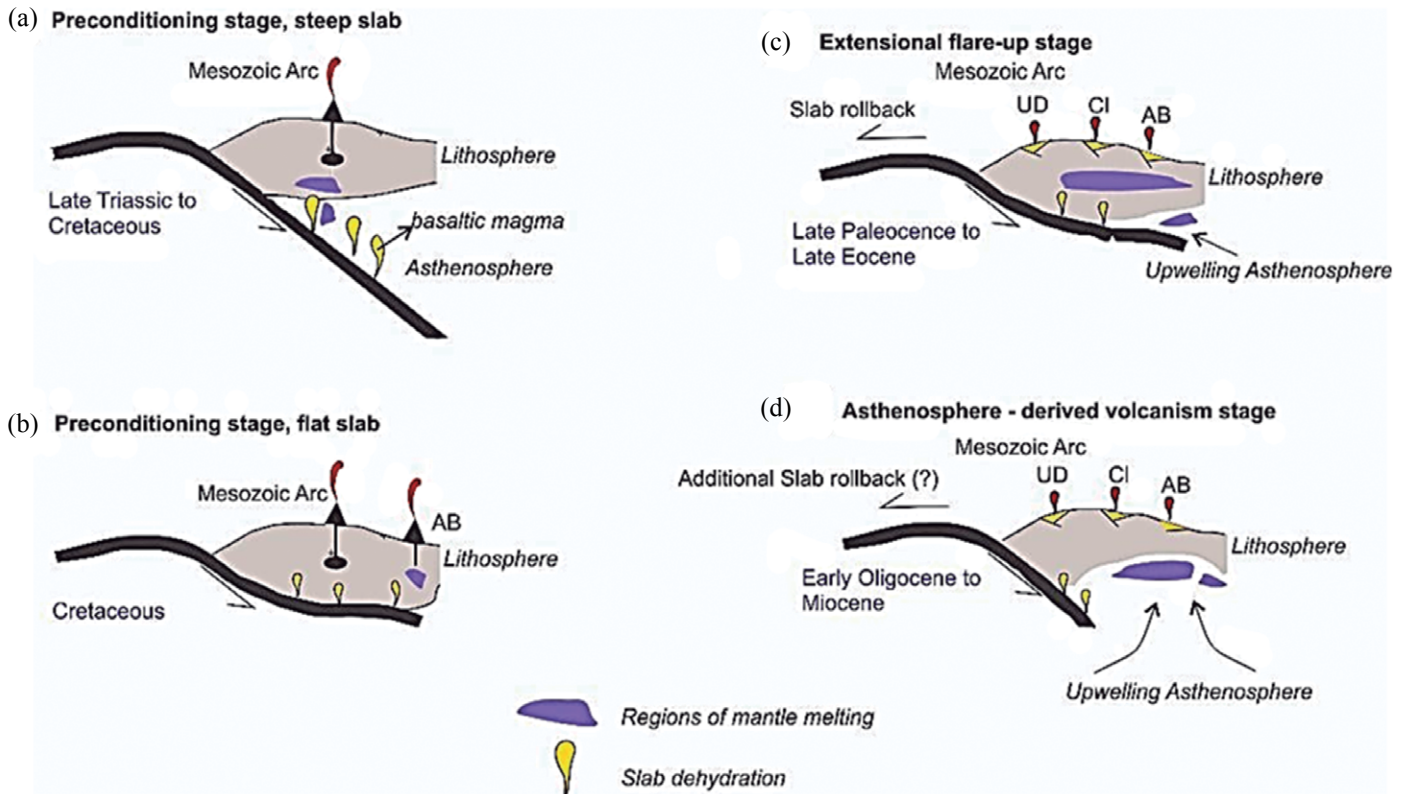


Figure 10. A view of evolution in the structural zones of Iran from late Triassic to Miocene UD= Urumieh-Dokhtar, CI=Central Iran, AB = Central Alborz, (A) Subduction of the oceanic crust in the upper Triassic to the Cretaceous along with the formation of volcanic arcs, (B) large-angle subduction is converted to flat subduction and local magmatism in the Alborz, (C) rollback of the subducted slab in the upper Paleocene and lower Eocene caused partial melting of the asthenosphere and uplift of asthenosphere and lithospheric window, (D) Continued extension in Oligocene to Miocene and formation of Qom formation (Verdel et al., 2011).

In the third stage (Eocene period), the rollback occurred in the oceanic crust. This phenomenon could be attributed to a number of factors including the rate of subduction, age of the sheet, the density difference between the plate and mantle, etc. (Heuret and Lallemand, 2005; Arfania, 2018). This results in the extension and thinning of the crust and uplift of the asthenosphere. Partial melting of hydrated peridotite occurred in the mantle due to pressure and heat reduction. The magma resulting from this melting was depleted in HFSE elements and was at the same time enriched with some other elements during the subduction caused by dehydration. At this stage, volcanic activities and shallow sea sediments formed in extensional environments (Figs. 10-c).

In the fourth stage (the beginning of the Oligocene), asthenosphere uplifting occurred due to the lithosphere thinning. At this time, the partial melting in the asthenosphere led to the formation of basaltic magma in the extensional basins. (Fig.10-d). these basaltic magmas were less contaminated due to crust thinning and mostly present the primary magma properties. (Plank and Langmuir, 1988; Glazner and Ussler, 1989; Ebrahimi et al, 2017).

Conclusion

According to the studies, the rock units in the area are divided into volcanic lavas and pyroclastic rocks. Volcanic lavas contain basalt, olivine basalt, andesitic basalt and basaltic andesite. In terms of chemical composition, the magma forming volcanic rocks in the Alamut region is alkaline. The normalized diagrams indicate that the basaltic rocks of the region are partially enriched with the asthenosphere mantle similar to the source of OIB with a partial melting degree of 12 to 15 and garnet lherzolite composition. Based on the graphical analysis and structural geology studies, the formation of rocks in the Alamut region has been related to the magmatism of continental rift zones. As a result of the deep faults, crust thinning, asthenosphere uplifting, local fractures formation by extensional phases (rifting), and partial melting in the asthenosphere, basaltic magma has formed in the extensional basin, which is less contaminated due to the crust thinning. The resulting basaltic magma

presents mainly the characteristics of the primary magma. The volcanisms of AVS are linear along these local extensional faults.

References:

- Abdel-Rahman, A. M., & Nassar, P. E. (2004). Cenozoic volcanism in the Middle East: petrogenesis of alkali basalts from northern Lebanon. *Geological Magazine*, 141, 545-563. <https://doi.org/10.1017/S0016756804009604>
- Allen, M. B., Ghassemi, M. R., Shahrabi, M., & Qorashi, M. (2003). Accommodation of Late Cenozoic oblique shortening in the Alborz range, northern Iran. *Journal of Structural Geology*, 25, 659-672. [https://doi.org/10.1016/S0191-8141\(02\)00064-0](https://doi.org/10.1016/S0191-8141(02)00064-0)
- Arfania, R. (2018). Role of supra-subduction zone ophiolites in the tectonic evolution of the southeastern Zagros Orogenic Belt, Iran. *Iranian Journal of Earth Sciences*, 10(1), 31-38.
- Berberian, M. (1982). The southern Caspian: A compressional depression floored by a trapped, modified oceanic crust. *Canadian Journal of Earth Sciences*, 20, 163-183. DOI: 10.1139/e83-015
- DePaolo, D. J., & Wasserberg, G. J. (1979). Neodymium isotopes in flood basalts from the Siberian Platform and inferences about their mantle sources. *Proceedings of the National Academy of Science of the United States of America*, 76, 3056-3060. <https://doi.org/10.1073/pnas.76.7.3056>
- Derakhshi, M., Ghasemi, H., & Sahami, T. (2014). Geology and Petrology of the Soltan Maydan Basaltic Complex in North- Northeast of Shahrud Eastern Alborz, north of Iran. *Scientific Quarterly Journal Geosciences*, 23(91).
- Ebrahimi, M., Esmaeili, R., & Aouizerat, A. (2017). New geodynamical model for the regional Tertiary extension during the Zagros orogeny: A transtensional arc? *Iranian Journal of Earth Sciences*, 9(2), 115-120.

- Haghnazar, S., Malakotian, S., & Allahyari, K. (2015). Tectono-magmatic setting of Cretaceous pillow basalts in the north part of the Alborz mountains in east of Guilan province (north of Iran): a part of ophiolite sequence or intra-continental rift? *Iranian Journal of Geosciences*, 24(94), 171-182.
- Haghnazar, S., Vosoughy Abebini, M., & Pourmoafi, M. (2009). Mantle source characteristics of Javaherdasht basalts (east of Gilan), Based on Attention to geochemical and isotopic features. *Iranian Journal of Geology*, 2(8), 95-102.
- Irvin, T., & Baragar, W. R. A. (1971). A guide to the chemical classification of the common volcanic rocks. *Canadian Journal of Earth Science Letters*, 8, 523-548. <https://doi.org/10.1139/e71-055>
- Jafarian, A. S. R., Imami, M. E., & Vosoughi Abedini, M. (2009). Petrology and Geochemistry of the Main Elements of the Basalt Collection of Sultan Sq. *Applied Geology Quarterly*, 4, 1-19.
- Jung, S. (1999). The role of crustal contamination during the evolution of continental rift-related basalts. A case study from the Vogelsberg area (central Germany). *Geolines*, 9, 48-58
- Le Bas, M. J., Le Maitre, R. W., Streckeisen, A., & Zanettin, B. (1986). A chemical classification of volcanic rocks based on the total alkali-silica diagram. *Journal of Petrology*, 27, 745-750. <https://doi.org/10.1093/ptrology/27.3.745>
- Le Roex, A. P., Dick, H. J. B., Erlank, A. J., Reid, A. M., Frey, F. A., & Hart, S. R. (1983). Geochemistry, mineralogy and petrogenesis of lavas erupted along the southwest Indian ridge between the Bouvet triple junction and 11 degrees east. *Journal of Petrology*, 24, 267-318. <https://doi.org/10.1093/ptrology/24.3.267>
- Meng, L., Li, Zh., Chen, H., Li, X., & Wang, X. (2012). Geochronological and geochemical results from Mesozoic basalts in southern South China Block support the flat-slab subduction model. *Lithos*, 127-140. <https://doi.org/10.1016/j.lithos.2011.11.022>
- Plank, T., & Langmuir, C. H. (1988). An evaluation of the global variations in the major element chemistry of arc basalts. *Earth Planet*, 90, 349-370. [https://doi.org/10.1016/0012-821X\(88\)90135-5](https://doi.org/10.1016/0012-821X(88)90135-5)
- Ritz, J. F., Nazari, H., Ghasemi, A., & Salamati, R. (2006). Active transtension inside central Alborz: A new insight into northern Iran-southern Caspian geodynamics. *Geology*, 34, 477-480. <https://doi.org/10.1130/G22319.1>
- Saunders, A. D., & Tarney, J. (1984). Geochemical characteristics of basaltic volcanism within back-arc basins In Marginal Basin Geology. *Special Publication of the Geological Society*, London, 16, 59-76. <https://doi.org/10.1144/GSL.SP.1984.016.01.05>
- Shervais, J. W. (1982). Ti-V plots and the petrogenesis of modern and ophiolitic lavas. *Earth and Planetary Science Letters*, 59, 101-118. [https://doi.org/10.1016/0012-821X\(82\)90120-0](https://doi.org/10.1016/0012-821X(82)90120-0)
- Talusani, V. R. (2010). Bimodal tholeiitic and mildly alkalic basalts from Bhir area, central Deccan Volcanic Province, India: Geochemistry and petrogenesis. *Journal of Volcanology and Geothermal Research*, 189, 278-290. <https://doi.org/10.1016/j.jvolgeores.2009.11.019>
- Verdel, C., Wernicke, B. P., & Hassanzadeh, J. (2011). A Paleogene extensional arc flare-up in Iran. *Tectonics*, 30, TC3008. <https://doi.org/10.1029/2010TC002809>
- Wang, Y. N., Zhang, C. J., & Xiu, S. Z. (2001). Th/Hf-Ta/Hf identification of tectonic setting of basalts (in Chinese). *Acta Petrologica Sinica*, 17(3), 413-421.
- Xu, Y. G., Ma, J. L., Frey, F. A., Feigenson, M. D., & Liu, J. F. (2005). Role of lithosphere-asthenosphere interaction in the genesis of Quaternary alkali and tholeiitic basalts from Datong, western North China Craton. *Chemical Geology*, 224, 247-271. <https://doi.org/10.1016/j.chemgeo.2005.08.004>
- Yaxley, G. M. (2000). Experimental study of the phase and melting relations of homogeneous basalt+peridotite mixtures and implications for the petrogenesis of flood basalts. *Contributions to Mineralogy and Petrology*, 139, 326-338. <https://doi.org/10.1007/s004100000134>
- Zaeimnia, F., Kananian, A., & Salavaty, M. (2011). Petrogenesis of Southern Amlash Alkaline Rocks in the South Caspian Sea, North of Iran. *Geosciences*, 78, 69-78.
- Zanchi, A., Berra, F., Mattei, M., Zanchetta, S., Nawab, A., & Sabouri, J. (2005). The early Mesozoic Cimmerian orogeny in the Alborz mountains, Iran. *Geophysical Research*, 7, 1607-7962.